The control and maintenance of desired flow patterns in bends of different orientations

D.Zhao[1], M.Abdulkadir[2], L.A. Abdulkareem[3], A.Azzi[4], F. Saidj[4], V. Hernandez Perez[5], R. Omar[6], B.N. Hewakandamby[6], B.J.Azzopardi[6*]

1 School of Engineering, London South Bank University, London, United Kingdom
2 Department of Chemical Engineering, Federal University of Technology, Minna, Niger State, Nigeria
3 Department of Petroleum Engineering, University of Zakho, Zakho City, Northern Iraq.
4 FGMGP/LTPMP, University of Sciences and Technology Houari Boumedien (USTHB), Algiers, Algeria
5 Department of Mechanical Engineering, National University of Singapore, Singapore
6 Faculty of Engineering, University of Nottingham, Nottingham, United Kingdom

ABSTRACT: Research into gas-liquid flow and bends can be motivated by the effect of the bend on the flow downstream of it which could alter the flow pattern occurring and the performance of downstream equipment. Alternatively, the interest might come from what occurs in the bend itself, there could be dryout of the film on the walls and consequent damage to the heat transfer equipment. Here we present measurements made with a number of accurate and fast responding sensors on three cases, two on the effect of the bend and one considering effects in the bend. The results, point to how to achieve certain flow patterns. Also recommendations are provided regarding the position of any sensor installed to determine flow pattern.

Keywords: Gas-liquid; Bends; Void fraction; Electrical tomography; Conductance

* Corresponding author e-mail: barry.azzopardi@nottingham.ac.uk

1. Introduction

Gas-liquid flow occurs in a variety of industries in many pieces of equipment and the linking pipework between them as well as in the environment. Of the diverse geometries through which gas-liquid flows pass, bends are an almost overlooked component. Yet they are central

to some equipment such as fired reboilers. It is also noted that volcanic conduits can include changes of direction, i.e., bends [1].

Now, bends, in many applications are just used to change the direction of a flow. However, it is important to understand the parameters required to define a bend. The first three parameters are the pipe diameter and the angle and radius of the bend. The angle of the bend, the angle between the inlet and outlet pipes, is most usually 90^0 or 180^0. Because it is gas-liquid flow that is being considered where gravity can cause stratification, the orientation of the inlet and outlet pipes must also be considered. It will be shown below that there are significant differences in going from horizontal to vertical and from vertical to horizontal. Finally there is the orientation of the bend. In the case of a 180^0 bend with both inlet and outlet pipes horizontal, whether the two pipes are in the same horizontal plane or whether the inlet or outlet pipe is on top can cause very noticeable difference to the flow as shown by Sakamoto et al. [2].

Control of the processes which affect the behaviour of gas-liquid flows in bends and its consequences can be passive or active. The former can involve activities such as design prior to construction or via modifications. Active controls demands continuous measurement of relevant variables and adjustments of flow rates or other parameters. Obviously, there is strong need for detailed knowledge of the distribution of the phases about the bend. This paper considers such information, that in the literature and particularly that generated by the authors of this paper. The implications for control will be discussed using two examples: (i) a fired reboiler with serpentine tubing and (ii) a novel combined bend/T-junction phase separator.

An extensive review of the available data on gas-liquid flow in bends is given by Azzopardi [3] which covers information available to that date. The effect of U and inverted U bends has

been considered by Golan and Stenning [4] and Takemura et al. [5] who noted that they act as phase separators because of the combined effect of centrifugal forces and gravity. In a U bend the two forces act in the same direction, usually sending the liquid to the outside of the bend and gas to the inside. In the inverted U-bend case the forces can act in opposite directions at lower liquid flow rates. However, at higher liquid flow rates, the centrifugal forces dominate and the liquid goes to the outside of the bend. Takemura et al. [5] confirm these trends from wall temperature excursions in electrically heated experiments. Golan and Stenning [4] report that the effect of the bend on phase distribution disappeared by 10 pipe diameters downstream of the end of the bend for the inverted U-bend case and 4 pipe diameter for the U-bend.

Fired reboilers are often used in refineries and other hydrocarbon processing plants to provide vapour where the boiling point of the hydrocarbon liquid is too high for steam to be used for heating. The tubing, usually of 0.1 to 0.15 m internal diameter, is fitted around the sides of the cylindrical or rectangular fire box. The flow is divided into several streams in parallel and each of these passes through an up and down serpentine arrangement. A major problem that can affect these units is “coking”. Dry-out of the wall film in annular or churn flow in the tubes can result in a local increase of wall temperature which can lead to a breakdown of the higher molecular weight hydrocarbon and deposition of carbon, in the form of coke, on the walls. If not detected this can build up and block the pipes. It tends to occur at lower mass flow rates. Indeed, a rule of thumb in the design of these units is that the mass flux through each tube should be at least 1000 kg/m^2s. Chong et al. [6] developed a model for these units based on the annular flow model of Hewitt and Govan [7] which took into account entrainment of liquid from the wall film and its redeposition back on to the film. For the serpentine geometry Chong et al. added the simplifying assumption that, at each U and inverted U bend, the drops entrained in the gas flow were deposited on to the film. This gave

conditions at which the film dried out, which was usually just before a bend, and showed that the flow rate at which dryout occurs increases with increasing heat flux. For heat fluxes usually employed, the value 1000 kg/m^{2}s was a conservative value. However, the calculations pointed out that if there was maldistribution between the parallel flow paths, those with lower flow rates could suffer dryout and, hence, coking. Industry sometimes uses a simple practical solution to prevent coking. The length of pipe just before the bend where dryout is most likely is insulated thus lowering the possibility of dryout.

Single or combinations of T-junctions, with one inlet and several outlets have been given serious consideration for use as gas-liquid phase separators. Azzopardi et al. [8] give details of a *partial* phase separator based on a bend/T-junction combination which was installed in a hydrocarbon processing plant and operated successfully until the plant shut down. It has been suggested that better positioning of the phases approaching the junction would improve separation efficiency. Sanchez-Silva et al. [9] have endeavoured to do this by positioning a branch pipe on the outside of a 90° bend with inlet and outlet pipes placed horizontally. They studied the effect of gas and liquid flow rate and the angle of inclination on the phase separation for slug flow approaching the bend. Increasing both gas and liquid flow rates increased the fraction of liquid taken off through the side arm. Baker et al. [10, 11] used control of a valve on one of the outlet lines of a multiple T-junction separator to optimise the efficiency of phase separation. They determined that different valve settings were required for this optimum separation and used an ECT system to identify the flow pattern.

Therefore, the knowledge of the flow phenomena in bends and their effect on downstream flow patterns is very important to many industrial applications involving multiphase flow. The flow distribution is affected by many factors such as the physical properties and velocities of fluids, the geometry (diameter, angle and curvature) and orientation of the bends. This paper is aimed to provide a more complete understanding on the effect on the

flow after the bends (effect of bend) and on the flow behaviour occurring in bends (effect in bend) through comprehensive experimental investigation employed advanced instrumentations. The experiments were conducted using air as gas phase and tap water or silicone oil (5 mPa s viscosity) as liquid phase. Bends with different geometries and orientations were examined. The work aims at providing useful data for the control and maintenance of desired flow patterns in and downstream of bends.

2. Review of previous work

Anderson and Hills [12], reported data on liquid film thickness, axial pressure profiles, gas velocity distribution, and droplet entrainment in the annular flow regimes in a vertical inverted 180^{o} return bend. The diameter and radius of curvature of the bend are 25 and 305 mm, respectively. They reported that an increase in film thickness on the inside of the bend can be attributed to the action of gravity and to the secondary flow existing in the gas phase. A change in flow pattern from annular to stratified flow in the bend at low liquid flow rates was observed. On the other hand, for the high liquid flow rates, a local maximum in the film thickness was seen on the inside and outside of the bend.

The distributions of water films and entrained droplets in air–water annular flows in 180^{o} horizontal bend were investigated by Balfour and Pearce [13] using sampling probes. The diameter and radius of curvature of the bend are 25 and 48.5 mm, respectively. They took a series of measurements with the probes positioned at 45^{o} intervals around the tube exit and at varying radii. They concluded that in those annular flows where the air speed is high, many of the entrained droplets are thrown very rapidly to the wall and that the entrained fraction tends to be negligible for high quality annular flows where the films are thin.

Using needle probes to measure the local void fraction around an inverted U-bend attached to a 50.8 mm internal diameter pipe in the case of froth flow enabled Hoang and Davis [14] to determine the slip ratio, which was found to be greatly increased at the bend exit, relative to the entry, for low velocity conditions. These values diminished slightly in the downstream flow pipe. Later, Takemura *et al.* [5] presented experimental results on the flow behaviour, pressure drop characteristics and dryout characteristics from the Joule heating of gas-water two-phase flows through U-shaped and inverted U-shaped bends, each having an internal diameter of 18 mm. They compared the results obtained from both bends and concluded that for the U-shaped bends, the gas phase flows along the inside of the bend, regardless of the flow rates of gas and water. Whilst in an inverted U-shaped bends, at lower gas and liquid flow rates, the tube wall at the outside of the bend at the angles of 150° to 180°varound the bend is in contact with the gas phase. They also reported that the inverted U-shaped bends have a wider safety region against dryout than the U-shaped bends.

Tingkuan *et al*. [15] studied the flow patterns in a vertical 180° bend using visual observation and physical measurements using electrical conductance probes. The diameter and radius of curvature of the bend are 21.5 and 305 mm, respectively. They compared their transition data to those reported by Mandhane *et al*. [16] and Weisman *et al*. [17]. They concluded that their data fitted the transition criteria from both sources well and that the major effect of the bend on the flow patterns is the considerable expansion of the stratified flow regime. This conclusion confirmed the earlier work of Anderson and Hills [12].

James *et al*. [18] investigated the effect of a 90^{o} horizontal bend on two-phase flow using computational and experimental studies. In their simulations using the Eulerian-Lagrangian method, they presented a suggestion as to whether droplets of a given size deposit in the bend. This they achieved by carrying out calculations using droplets in the size range of 10 to 500 μm diameters.

Experimental work in a horizontal 180° bend using air and water as the working fluids was presented by Sakamoto *et al*. [2]. The diameter and radius of curvature of the bend are 24 and 135 mm, respectively. They employed the conductance type void probe to measure the liquid film thickness and an L-shaped stainless steel sampling tube to measure the local droplet flow rate. They reported the distributions of annular liquid film thickness and the local drop flow rate in the gas core in a straight pipe and at the end of three U-bends at horizontal to horizontal (upward), vertical upward, 45^{o} upward to the horizontal. They claimed that the local flow rate of droplets in the gas core in horizontal pipe flow reaches a minimum near the lower wall of the pipe and a maximum near the upper wall.

The effect of 90^{o} bends on two-phase air–silicone oil flows was investigated by Abdulkadir *et al*. [19] using advanced instrumentation, electrical capacitance tomography (ECT), wire mesh sensor (WMS) and high speed camera. They mounted the ECT probes upstream of the bend while WMS was positioned immediately upstream or immediately downstream of the bend. The downstream pipe was maintained horizontal whilst the upstream pipe was mounted either vertically or horizontally. The bend (R/D) was made of transparent acrylic resin. The superficial velocities of the air that they considered ranged from 0.05 to 4.73 m/s and for the silicone oil from 0.05 to 0.38 m/s. From an output from the tomographic equipment, they identified flow patterns using both the reconstructed images as well as the characteristic signatures of probability density function (PDF) plots of the time series of cross-sectional averaged void fraction.

The behaviour of film fraction within a vertical 180^{o} bend using air and water as the operating fluids has been investigsted experimentally by Abdulkadir *et al*. [20, 21]. The diameter and radius of curvature of the bend are 127 and 381 mm, respectively. In the first paper they reported on measurements of cross-sectional film fraction using conductance ring probes placed at 17 pipe diameters upstream of the bend, 45^{o}, 90^{o} and 135^{o} into the bends and

21 pipe diameters downstream of the bend. They reported that the average film fraction is higher in straight pipes than in bends and that the condition for which the liquid goes to the outside or inside of the bend can be identified based on a modified form of Froude number, a proposal first made by Oshinowo and Charles [22]. The second paper [21] described measurements of film thickness distributions of film thickness around the pipe circumference at different points around the bend. They employed air superficial velocities of 3.5 to 16.1 m/s and water superficial velocities from 0.02 to 0.2 m/s. The liquid film thickness distribution in the bend was measured with pin and wire probes. With the former for measuring thin films (up to 2.5 mm) outside the bend while the latter for thick liquid films inside the bend. These measurements have been supplemented by visual observation.

Kerpel *et al.* [23] investigated the behavior of two-phase flow up- and downstream of a sharp return bend. They used a return bend with a radius of curvature of 1 mm and an inner diameter of 8 mm. The refrigerant used is R134a; the mass flux was varied between 200 to 400 kg/m^2 and the vapor quality varied between 0 and 1. The bend orientation is vertical. Upward flow as well as downward flow through the bend was studied. Eight capacitance sensors were placed at several locations upstream and downstream of the return bend. The series of void fraction from the sensors were compared in order to determine the presence and extent of the bend effect. They concluded that the disturbance due to the return bend stretches out, to at least 21.5 tube diameters downstream of the bend. Upstream of the bend, an effect was absent for downward flow, for upward flow a limited effect was observed.

Experimental measurements of single-phase and two-phase frictional characteristics and associated observations of flow patterns associated with a 90^o bends were discussed in the paper by Hsu *et al.* [24]. The two bends have inner diameters of 5.5 and 9.5 mm with tube curvature ratio (2R/D) of 5.4 and 4.2, respectively. The bends were installed upward, horizontal or downward arrangement. They found that for single-phase flow, the bend friction

factor was always greater than that of the straight tubes at the same Reynolds number. On the other hand, the bend friction factor values for a pipe diameter of 9.5 mm with smaller curvature ratio are greater than those from a diameter of 5.5 mm. the resultant two-phase frictional pressure drops of 90^{o} bend were well predicted by the correlation of Sanchez-Silva [9]. For the two-phase frictional pressure gradient, the upward arrangement is greater than that of the horizontal arrangement due to swirled motion and liquid flow reversal.

Yadav *et al.* [25] reported experimental investigations concerning air–water two phase flow through a 2.25 mm circular mini-channel U-bend. They established the influence of radius of curvature by developing 2 mini-channel U-bends with radius of curvature as 6 mm and 12 mm. A T-junction was used as mixing geometry for air and water. The superficial gas and liquid velocities were in the range 0.0419–0.4192 m/s. At these flow rates, five flow patterns were identified including plug, slug, bubbly, bubbly-plug and deformed plug. Flow pattern transition maps were developed as a function of radius of curvature. The influences of radius of curvature on hydrodynamics of Taylor bubble flow such as void fraction, liquid hold up, Taylor bubble velocity, Taylor bubble and liquid slug length was investigated. The radius of curvature with other flow parameters was found to have significant effect on two-phase flow patterns, its transition boundaries and hydrodynamics of Taylor bubble flow.

At Cranfield University, experiments have examined flow in a serpentine geometry with vertical pipes [26, 27]. The arrangement consisted of four pipes joined by U and inverted U bends starting with an upwards flow. Measurements were made on the first down and second up sections at 5, 30 and 46 pipe diameters from the preceding bend using Wire Mesh Sensor and local conductivity probes for film thickness which were mounted at very 90° around the circumference. It was reported that though there was an obvious asymmetry in the circumferential film thickness profile at the 5D position, this was hardly noticeable by the 30D station.

3. Experimental instrumentation

A number of different of instruments and measurement sensors were used in this work. They are described below.

3.1 Electrical Capacitance Tomography (ECT)

A detailed description of the theory behind the ECT technology is described by Huang [28], Zhu et al. [29] and Hunt et al. [30]. The method can image the dielectric components in the pipe flow phases by measuring rapidly and continually the capacitances of the passing flow across several pairs of electrodes mounted uniformly around an imaging section. Thus, the sequential variation of the spatial distribution of the dielectric constants that represent the different flow phases may be determined. In this study, the ECT system (Fig.1) supported by TomoFlow limited, had been previously used by several researchers. Details can be found in Azzopardi et al. [31], Abdulkareem [32], Abdulkadir et al. [19].

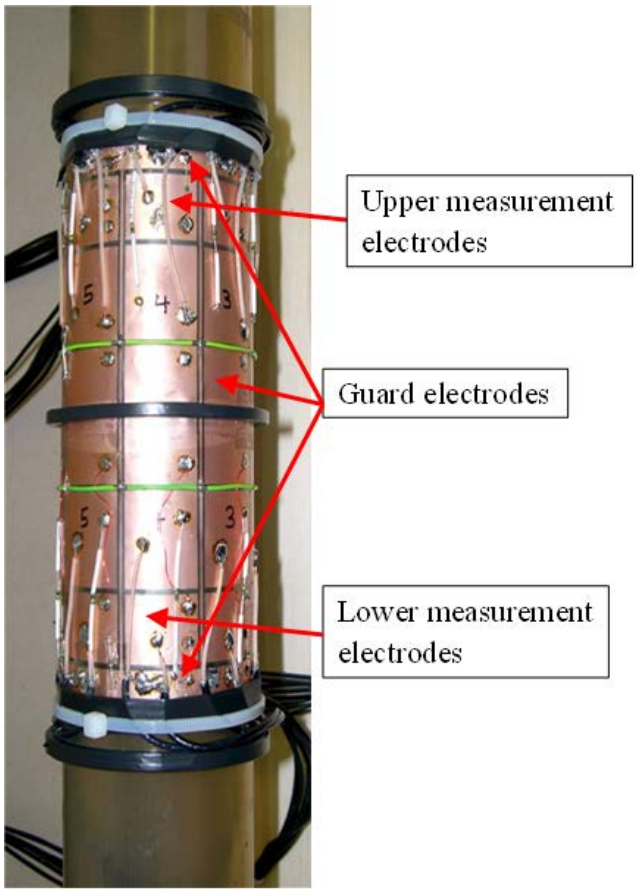

Fig. 1 ECT sensor

A simplified version of the approach has been proposed [33] which can be used to idenify flow patterns for a given set of flow rates.

3.2 Wire Mesh Sensor (WMS)

The capacitance WMS sensor (Fig.2) described in detail by da Silva et al. [34] can image the dielectric components in the pipe flow phases by measuring rapidly and continually the capacitances of the passing flow across several crossing points in the mesh. It consists of two planes of 24 stainless steel wires with 0.12 mm diameter, with a 2.78 mm wire separation within each plane and 2 mm axial plane displacement. It was noted that since the square sensor is installed in a circular tube, only 440 of the total 576 wire crossing points are within the radius of the tube. During the experiments, the transmitter lines are pulsed one after another. By measuring the signal of all crossing orthogonal receiver wires, the local capacitance at the crossing points in the mesh is determined. This capacitance signal is a measure for the amount of silicone oil, and thus indicates the local phase composition in the grid cell. Systematic tests have been carried out to test the accurracy of the WMS/ECT. Sharaf et al. [35] made simultaneous measurements with WMS and nuclear absorption (gamma). The beam of the latter was positioned immediate below each of the wires in turn. The chordal average was obtined from both instruments and good agreement was achieved. Azzopardi et al. [36] made simultaneous measurements with WMS/ECT. Excellent agreement was found in the comparison of the time and cross-sectionally averaged void fractions.

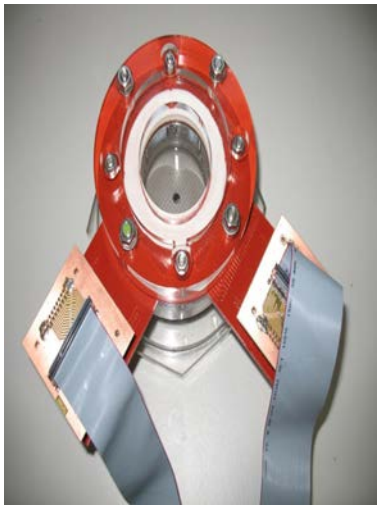

Fig. 2 WMS sensor

3.3 Ring probes

Cross-sectionally averaged void fraction in two-phase gas-liquid mixtures can be measured by two flushed mounted parallel ring probes. They were first employed by Asali et al. [37], while Andreussi et al. [38] and Tsochatzidis et al. [39] developed the theoretical bases regarding the response of this electrode configuration. Fossa [40] compared the phase distribution results measured with two flushed mounted parallel ring probes for annular, stratified and bubble flow with the theoretical data available in the literature. The probes used in this work consist of two stainless steel ring electrodes mounted in acrylic resin housing (Fig.3). They were carefully manufactured so that the electrodes had the same diameter as the test section. Details of the geometry can be found in Saidj et al. [41].

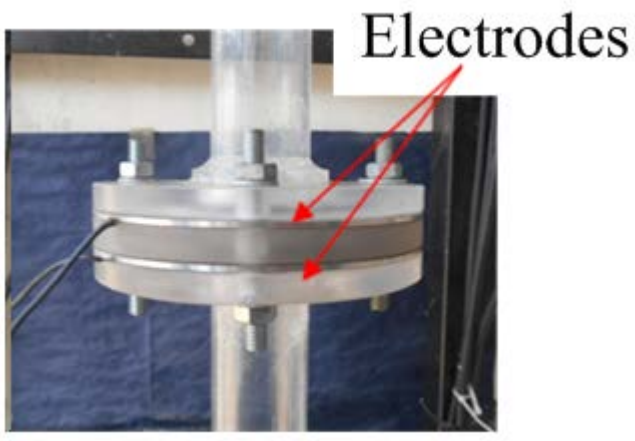

Fig. 3 Ring probes

3.4 Pin probes

For gas–liquid annular flow in which the liquid is electrically conducting, liquid film thickness can be determined by the measurements of the electrical conductance between two electrodes in contact with the liquid film. The measured liquid film thickness is assumed to be the value at the mid-point between the centres of the electrodes. Different electrode geometries of such as needle probes, parallel wire probes and flush mounted pin probes have been reported by researchers over the last decades [42-45]. Flush mounted pin probes are suitable for measuring very thin liquid films, typically up to 2.5 mm. If care is taken in the mounting of probes, the method is virtually non-intrusive. The electric field is very weak away from the pipe surface and has a negligible contribution to the passage of current. The response of the pin probe is initially linear to the thickness of the liquid film (typically up to 2 mm) and then asymptotically flattens to a uniform value to the thicker liquid film. This phenomenon is called probe "saturation". When the probe is saturated, its output signal is not sensitive to the change of liquid film thickness. To enlarge the range of measurement, the diameter and separation of pins needs to be increased. However, the greater the spacing, the more averaged is the result over space. To obtain an optimum measurement of the liquid film thickness therefore, a balance must be struck between range of operability and local character of the measurement [29]. The pin probe used in this work is shown in Fig.4. The probe consists of 20 pairs of electrodes made of 1.5 mm diameter stainless steel welding rods. Every pair of pins is spaced 15^{o} away from the neighbour pair while the space in the same pair is 5^{o}. The flow of electrical current from a transmitter in one probe to the neighbour receivers and transmitters (cross–talk) will decrease the spatial resolution of the sensor (Belt 2006), and thus increase the measurement errors of the liquid film thickness. To reduce the

effect of cross–talking, the signals from the 20 pair of pins were taken as 4 groups: 1, 5, 9, 13 and 17 in group A; 2, 6, 10, 14 and 18 in group B; 3, 7, 11, 15 and 19 in group C and 4, 8, 12, 16, and 20 in group D. Details of probe calibration can be found in [29-31].

Fig.4 Pin Probes

3.5 Parallel wire probe

When the liquid film thickness is beyond the measurement range of the pin probes, parallel wire probe can be used. Wire probes were originally used by [43-47]. According to Brown et al. [48] these probes give a linear response versus liquid film thickness and allow more localised measurements of thicker films to be carried out. The intrusive wires, however, may cause the perturbation to the flowing film. The disturbance can be minimised by the use of very thin wires [48]. A more significant disturbance may occur when the probe has to work in

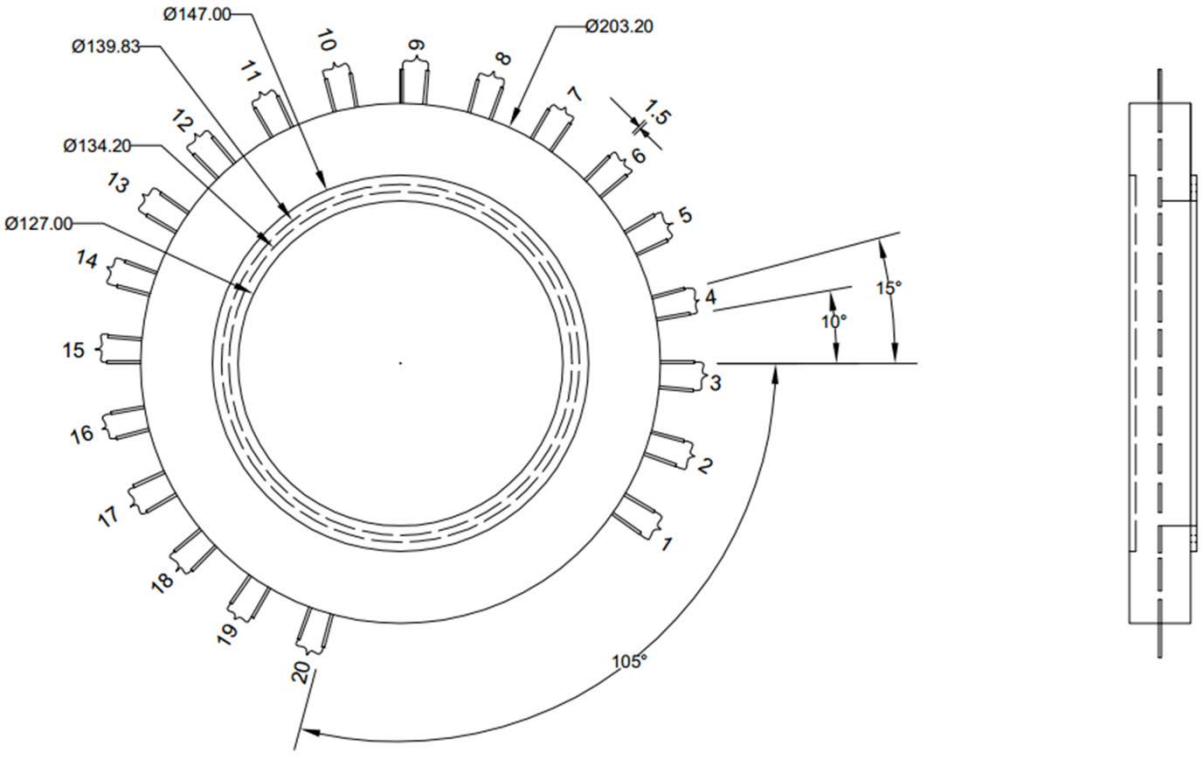

a wavy film. When the liquid height decreases, a thin liquid layer sticks to the probe which might indicate a liquid level higher than the actual level, thus introducing a certain amount of lag in the dynamic response of the probe. This phenomenon was investigated experimentally

[36] who reports these errors to be negligible and that the response of the probe is almost instantaneous. In this work, the parallel-wire probe (Fig.5) used to measure liquid film thickness at the bottom of the bend is the same type employed by [26, 28, 31, 37, 38]. It has five pairs of stainless steel wires with the diameter of 0.33 mm stretched along the chords of the cross-section of the pipe. The spacing between the two wires of each pair is of 5 mm and the distance between the neighbour pairs is 20 mm, with the central pair placed symmetrically about a vertical diameter. Details of the electronic circuit and probe calibration can be found in [31, 37].

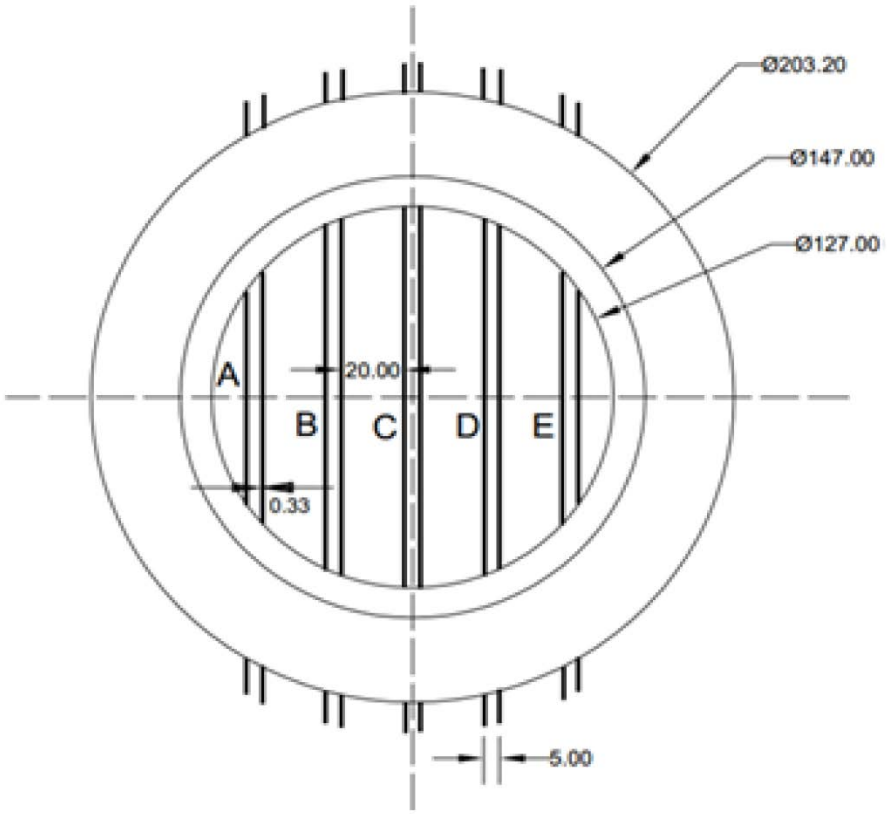

Fig.5 Parallel wire probe

4. Results and discussion

4.1 Horizontal to vertical upwards 90^o bend with ID of 34 mm

Tap water drawn by a pump from a storage tank is injected into a mixer where it is mixed with the air supplied from a compressor. The air-water mixture flows through a horizontal pipe, a horizontal to vertical 90^o bend with a curvature of 5, a vertical pipe and finally to the

storage tank, where the air and the water are separated. All the pipes have the same internal diameter of 34 mm and a length of 150 diameters of the pipe to ensure full development of flow. The water is recirculated and the air is released to the atmosphere. Nine ring probes shown in Fig.3 were placed along the test section. Three before the bend, at 1175, 660 and 145 mm, and six after the bend, at 145, 660, 1175, 1690, 2205 and 2720 mm respectively from the bend. The position of the first probe was 3935 mm from the mixer. More details of rig setup and probe calibration can be found in [24].

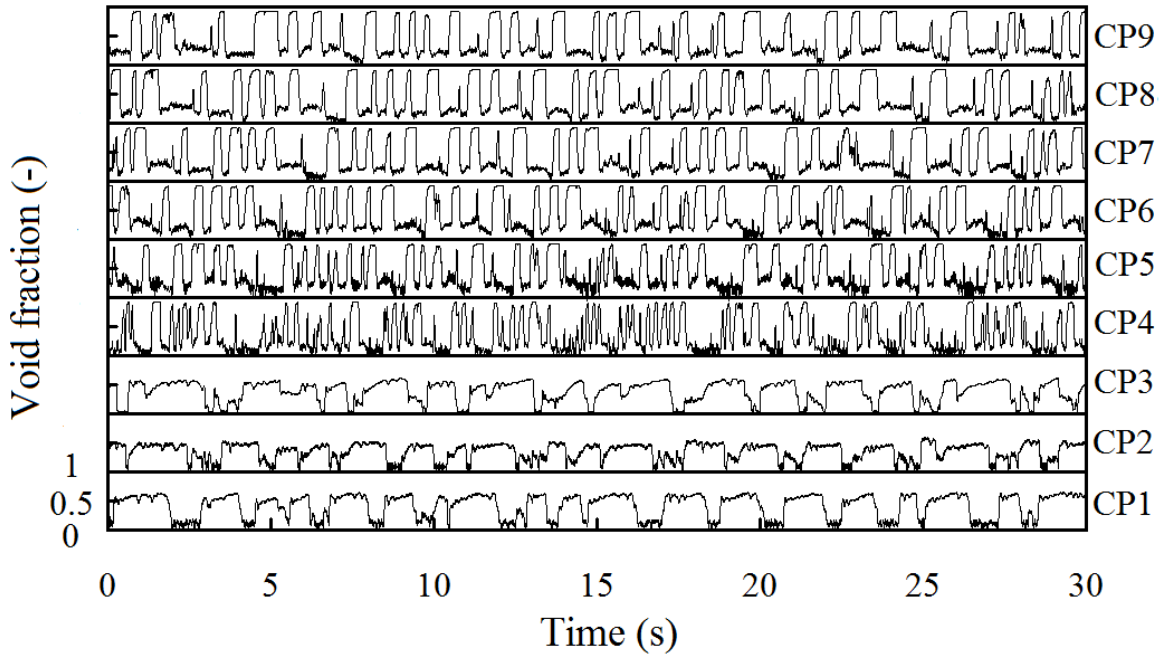

Fig. 6 Time series of cross-sectionally average void fraction along the test section (liquid superficial velocity = 0.3 m/s, gas superficial velocity = 0.32 m/s)

Figure 6 shows an example of the average void fraction time series obtained from the nine conductance probes (CP) in the flow line and in the riser (CP1 to CP9). The superficial velocities are 0.3 and 0.32 m/s for the liquid and the gas respectively. It is obvious that the bend affects the flow behaviour, which can be noticed in the time traces of the first conductance probe just downstream the bend. The flow then, tends to re-establish itself from practically the probe (CP7) where the time series remain the same.

Based on the work of Jones and Zuber [39], the flow regime can be quantitatively identified by examining the signature of probability density functions (PDF) of the cross sectional averaged void fraction data. For example, slug flow is featured by twin peak PDF, one at low void fraction corresponding to the void fraction in liquid slug while the other at high void fraction representing Tylor bubble. The analysis of PDF characters provide clear evidence that stratified plug, wavy and slug flows were developed in the flow line while slug and churn flows occurred in the riser when the gas and liquid superficial velocities were operated from 0.3 to 4 m/s and from 0.21 to 0.91 m/s respectively. This is also confirmed by direct

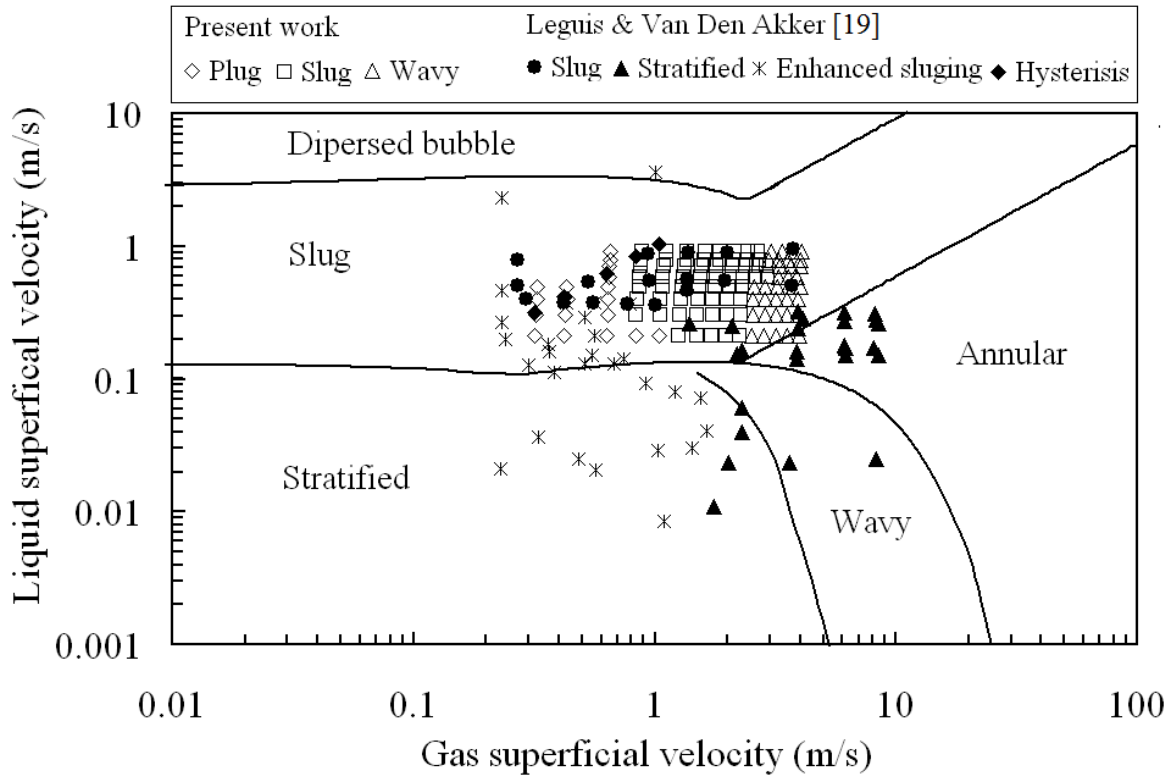

visualisation. The flow pattern maps of up- and down-streams of the bend are shown in Fig.7 and Fig.8 respectively.

Fig.7 Flow pattern map in the flow line upstream the 90°bend [24]

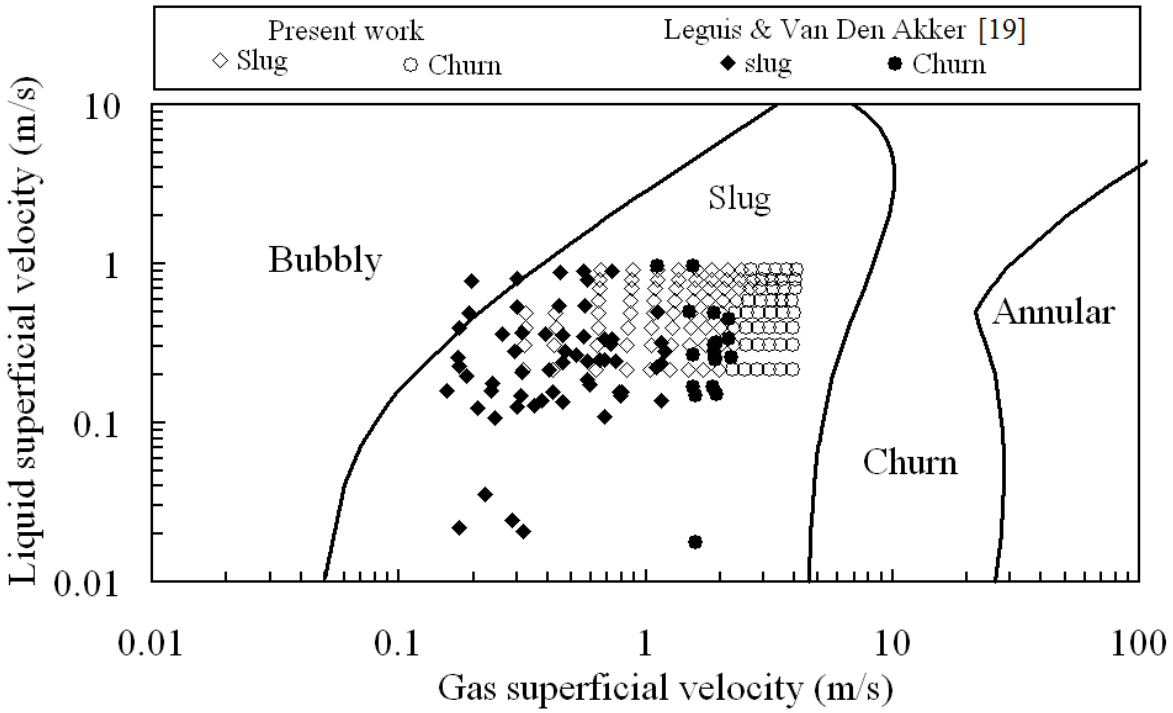

Fig.8 Flow pattern map in the riser downstream of the 90° bend [24]

A flow is considered fully developed when its configuration does not change after it travels a certain distance. In order to follow and quantify the minimum distance necessary for the development of the flow after the 90° bend, the Probability Density Function (PDF) of the void times series obtained from the six conductance probes after the bend (CP4 to CP9) are plotted and analysed. The six probes are located 145, 660, 1175, 1690, 2205 and 2720 mm respectively 4, 19, 35, 50, 65 and 80 pipe diameters downstream the bend respectively. The plots corresponding to the minimal liquid and gas superficial velocities combinations are shown in Figs. 9 and 10. It appears from these figures that the shapes of the PDFs are changing along the downstream pipe of the bend and remain the same from the fourth conductance probe from the bend (CP7), situated 50 pipe diameters length from the bend. It is worth to note that this recovery length is in the order of that found by [40]. Indeed these latter, from the analysis of pressure drop of a combination of pipe components positioned

horizontally, found that the two-phase flow is recovered at about 10 to 50 pipe diameters downstream the 90° bend depending on the flowrates.

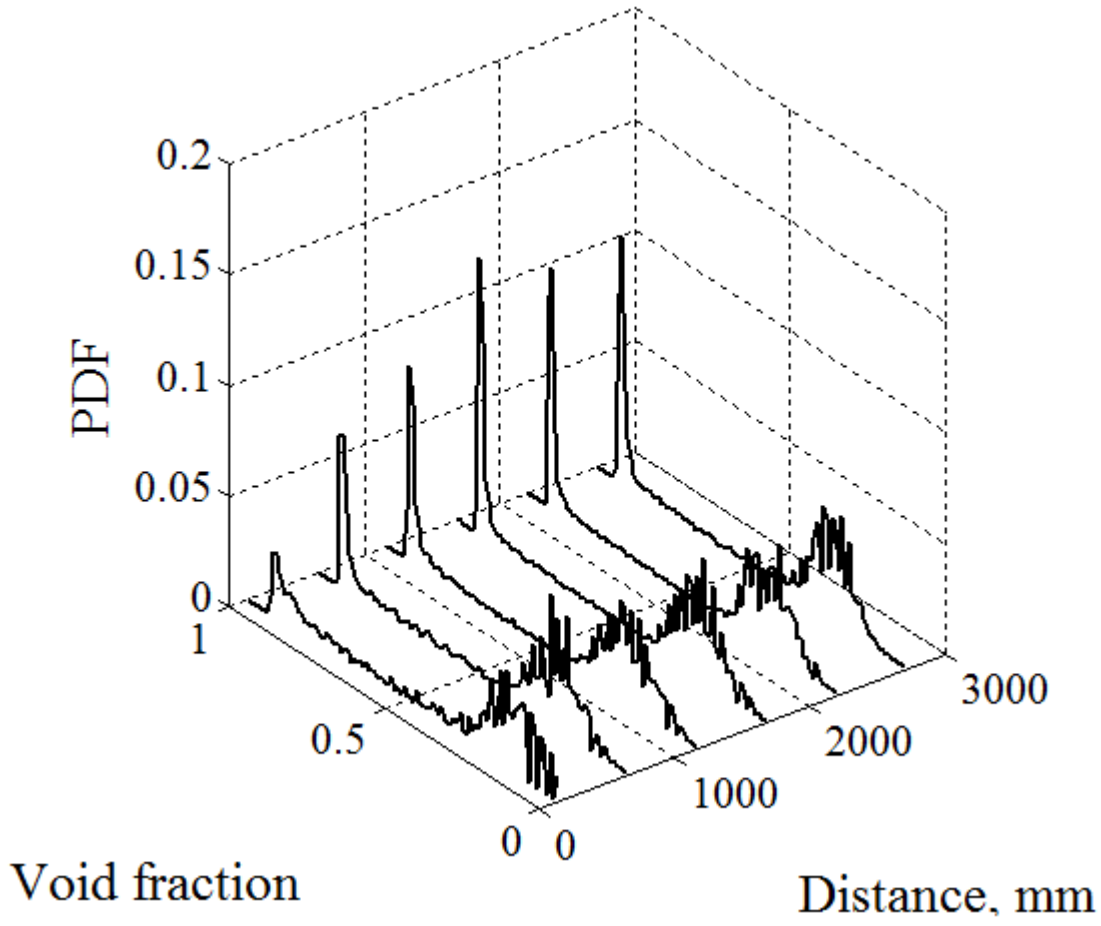

Fig.9 Probability Density Function of the void fraction time series downstream the bend (liquid superficial velocity = 0.3 m/s, gas superficial velocity = 0.32 m/s)

If the characteristic frequency obtained from the Power Spectral Density of the time series of void fraction are considered for the horizontal as well as the vertical pipe, it is seen in Fig. 10 that for the lower gas superficial velocities the frequencies are substantially the same upstream and downstream of the bend. The liquid superficial velocity was 0.49 m/s in this case. Similar results at higher and lower liquid superficial velocities have been presented elsewhere [36]. This is the persistence of frequency concept introduced by Azzopardi et al. [xx] and considers that if the is slug flow in the horizontal pipe this will continue with the same frequency in the vertical pipe after the bend. In

contrast, when the flow in the horizontal pipe is stratified, there is of necessity a change in flow pattern in the vertical pipe and the frequency changes across the bend.

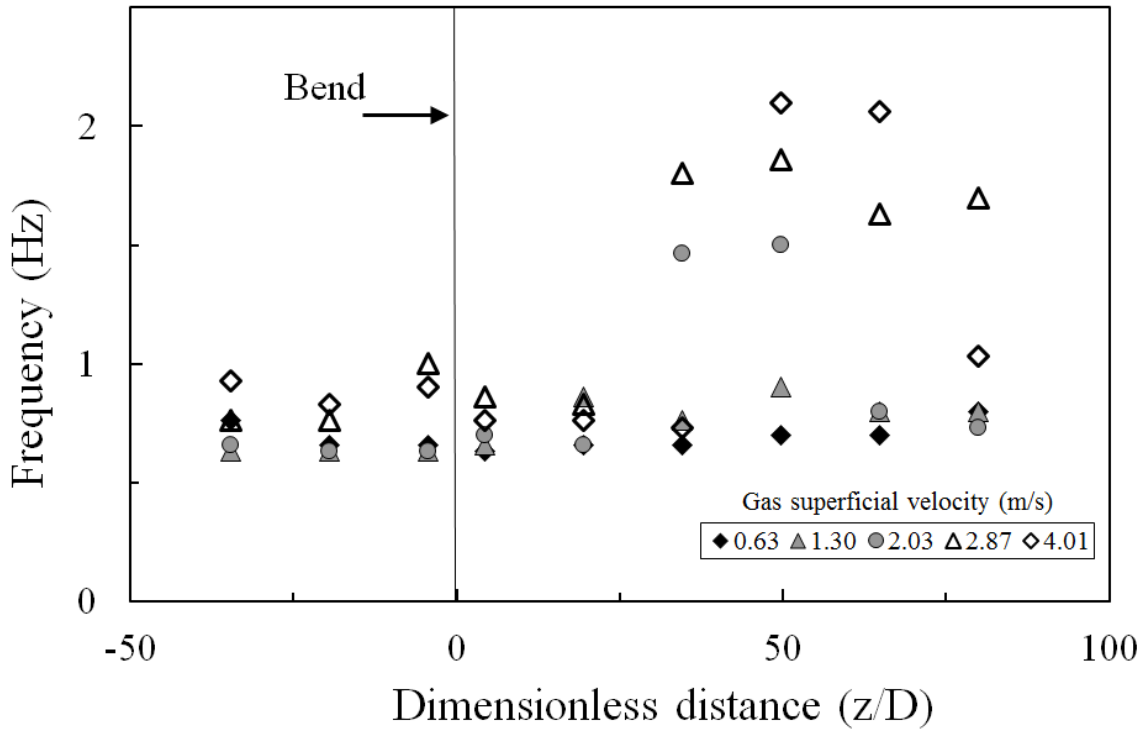

Fig.10 Axial variation of characteristic frequency. Liquid superficial velocity = 0.49 m/s

4.2 90^{o} bends in series (vertical to horizontal then horizontal to horizontal)

Experiments were carried out on the effect of two orientations of bends. Initially, a vertical to horizontal bend was investigated with measurements made just before and just after the bend. Subsequently, a more extensive arrangement was employed with a 4.5 m long vertical pipe followed by a vertical to horizontal bend 9.2 m long horizontal pipe leading to a bend in the horizontal plane and a further 5.5 m of horizontal pipe. In both cases the pipe diameter was 67 mm and the fluids utilised were air and a silicone oil with viscosity of 5 mPa s. The ECT and WMS techniques were used. Data collection from the ECT was synchronised with that of the WMS by sharing one trigger command. A sampling time of 60 seconds was

employed and sampling rates of 200 Hz (ECT) and 1000 Hz (WMS) utilised. The bends were manufactured from transparent acrylic resin and polished to enable high quality images to be obtained. Tests showed that the length of 4.5 m (66 pipe diameter) of vertical pipe was sufficient to provide a reasonably developed flow at the entrance to the bend [41-43]. In these experiments the ECT was always placed at 5D upstream of the bends, while the WMS was located at 1, 10 40, 69, 98 and 128 diameters from vertical to horizontal bend and 10, 40, 69 and 75 diameters from the horizontal to horizontal bend.

Time averaged void fraction (sometimes considered as its compliment, liquid hold up) is important in calculation of pressure drop in piping. For a given liquid superficial velocity, it increases with gas superficial velocity. If the values obtained from the data of ECT and wire mesh sensor for upstream and downstream of the bend, respectively, are considered it is seen that at intermediate liquid superficial velocities, 0.157 and 0.314 m/s, the mean void fractions follows the same trend and there is good agreement between the values upstream and downstream of the bend. However, at higher and lower liquid superficial velocities, 0.052 and 0.524 m/s, the void fractions decrease after the mixture passes the bend. This difference is probably due to the change of flow patterns caused by the change in direction of the effect of gravity. In stratified flow the controlling force is gas shear whilst in slug flow part of the liquid is pushed along by the gas.

As discussed in the previous section, the time series of cross-sectional average void fraction shows many essential features of the flow. Examples are given in Fig. 11 of such data taken with the WMS mounted just before and just after the vertical to horizontal bend. These are from a liquid superficial velocity of 0.38 m/s and the gas superficial velocities of 0.05 and 0.71 m/s. The effect of the bend on the flow behaviour can be clearly seen from the figure. For the lower flow rate, the flow patterns upstream of the bend is bubbly flow and stratified wavy downstream of it. In contrast at the higher gas flow, there is slug flow in the vertical

pipe whilst downstream of the bend there is plug flow with its large gas bubbles separated by a liquid layer [24].

(a)

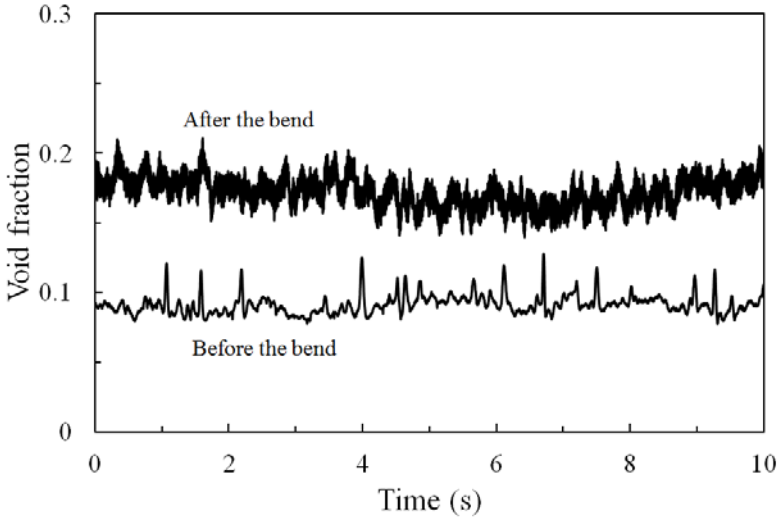

(b)

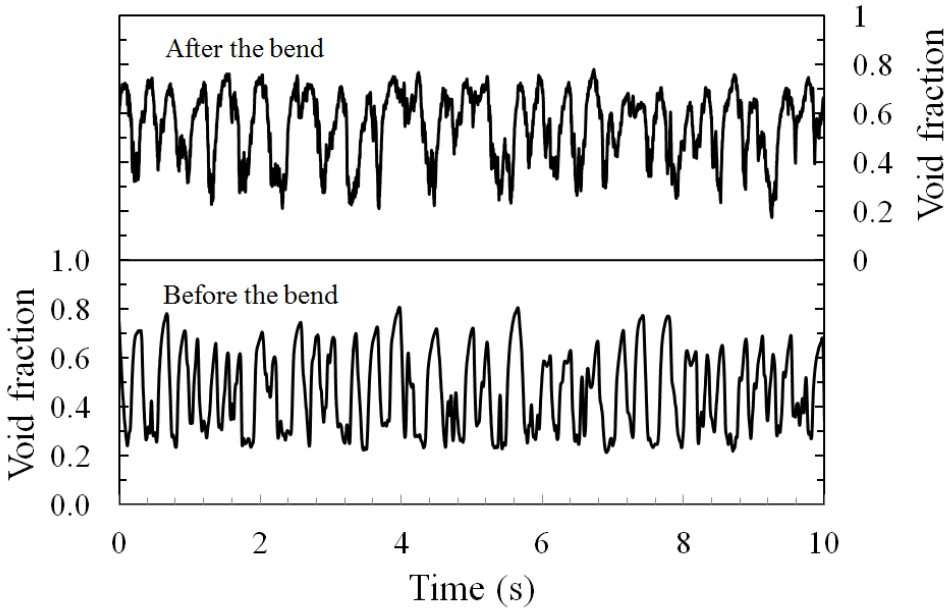

Fig.11 Time series for void fractions at upstream and downstream of the bend (liquid superficial velocity of 0.38 m/s and gas superficial velocities of (a) 0.05 and (b) 0.71 m/s)

The main flow patterns observed for the vertical test section during this study are bubbly, spherical cap bubbles, slug, churn flows in the vertical pipe and stratified, wavy stratified,

plug and slug flows in the horizontal lengths. The superficial velocities for the gas were from 0.045 to 3.21 m/s and whilst those for the liquid were from 0.15 to 0.53 m/s. At lowest gas superficial velocity studied, 0.05 m/s, the flow pattern in the vertical pipe was bubbly flow. At the phases passed around the bend to the horizontal section, the liquid phase drained to the bottom of the pipe due to the effect of gravity and stratified flow results as shown in Fig.15 was dominant for the whole length of the horizontal section. When the gas superficial velocity increased to 0.18 m/s, the flow in the vertical section became of the cap bubble type while slow moving slugs were observed in the horizontal section. The liquid level was high enough to bridge the pipe to form plug flow. The body of those slugs contained a limited number of air bubbles. Slugs increased in length as they moved down the horizontal pipe. At higher gas superficial velocity, slug flow became dominant in the vertical pipe. As the slugs approach the bend, the liquid phase was moved to the outside of the bend at first due to the effect of the centrifugal force. Further round the bend, the gravitational pull drained the liquid to the inside of the bend leaving dry patch on top, until a new slug unit covered the dry zone occupied by the gas phase. In this case the flow in the horizontal section near the bend was stratified with slightly disturbed interface; while hydrodynamic slugs formed at ~55D downstream the bend. The body of the slug at these conditions contained more dispersed bubbles. One important, but often overlooked, feature is that some slugs are more likely to break up before leaving the test section. At the maximum liquid and gas superficial velocities (liquid superficial velocity = 0.53 m /s ,gas superficial velocity = 3.21 m/s) the flow in the riser was churn while stratified wavy was dominant up to ~55D downstream the bend in the horizontal section, then slug flow become dominant for the rest of the pipe length.

These direct visual observations were confirmed by ECT/WMS images of cross-section distribution of the phases and data of the PDF of the void fraction time series obtained from ETC and WMS sensors. These displays of the evolution of the flow are shown in Figs. 11 and

12 respectively for a lower flow condition, and in Figs 13 and 14 for the highest flow rates studied, liquid superficial velocity of 0.53 m /s and gas superficial velocity of 3.21 m/s.

It is noteworthy that the PDF signatures of the void fraction time series in the vertical pipe from Fig.14 right bottom graph and that the PDFs signature of churn flow in the riser and the slug flow in the horizontal section are similar in shape. This due to that the hydrodynamic slugs formed at these conditions contain a very high dispersed bubble population where the gas hold up reaches a maximum value of around 0.48.

Both the ECT and WMS systems can produce phase distribution images of fluids inside the pipe. The images obtained from the WMS are shown relative to the position where they were taken in Fig.12 where blue represents the liquid phase and the red gas. This is for a lower flow rates, gas superficial velocity of 0.05 m/s and liquid superficial velocity of 0.15 m/s. As seen the flow is bubbly at the top of the vertical section but is stratified in the horizontal pipe. This is confirmed by the equivalent plots of the PDFs of the cross-sectionally averaged void fraction illustrated in Fig. 13. Downstream of the horizontal to horizontal bend the PDFs show a two peak shape. These normally would be associated with slug flow, however, direct observation indicate that at the lower void fraction conditions, the liquid level did not touch the top of the pipe and were more a manifestation of a wavy stratified flow. Figs. 14 and 15 are the corresponding plots for higher flow rates, gas superficial velocity of 0.55 m/s and liquid superficial velocity of 0.45 m/s. Here the flow pattern is slug flow at the top of the vertical pipe and in the horizontal pipe.

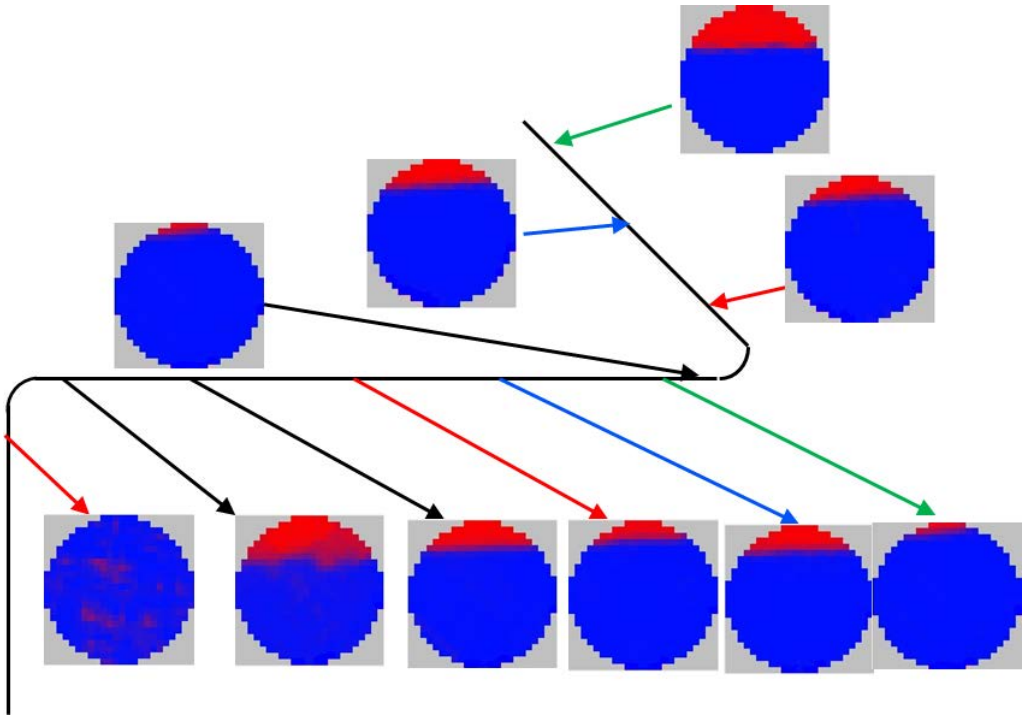

Fig. 12 Tomographic images from positions along the pipe system. Liquid superficial velocity = 0.15 m/s and gas superficial velocity = 0.05 m/s.

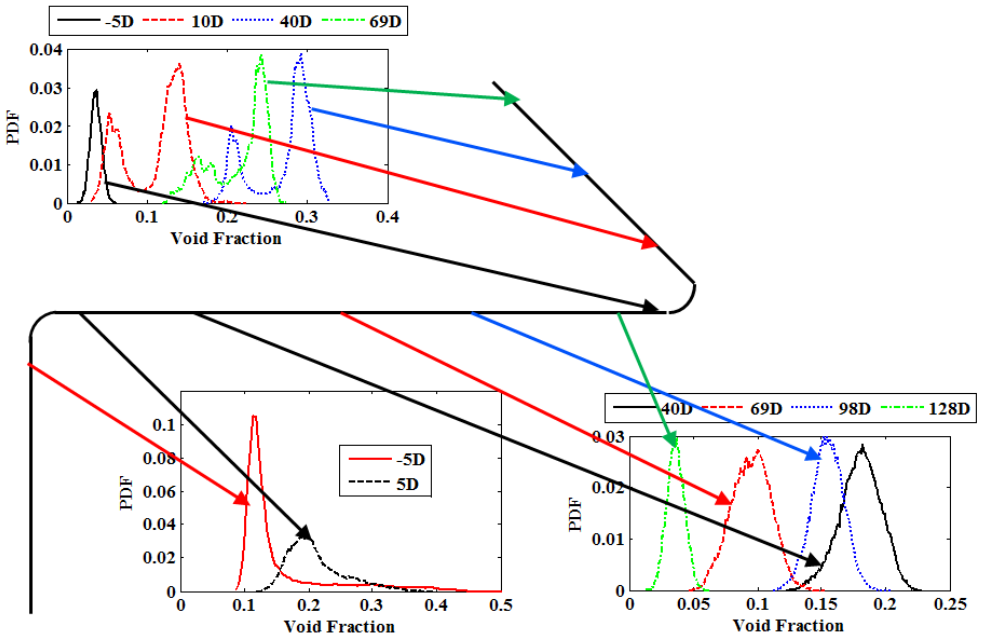

Fig.13 Probability Density Function of void fraction time series positions along the pipe system. Liquid superficial velocity = 0.15 m/s and gas superficial velocity = 0.05 m/s.

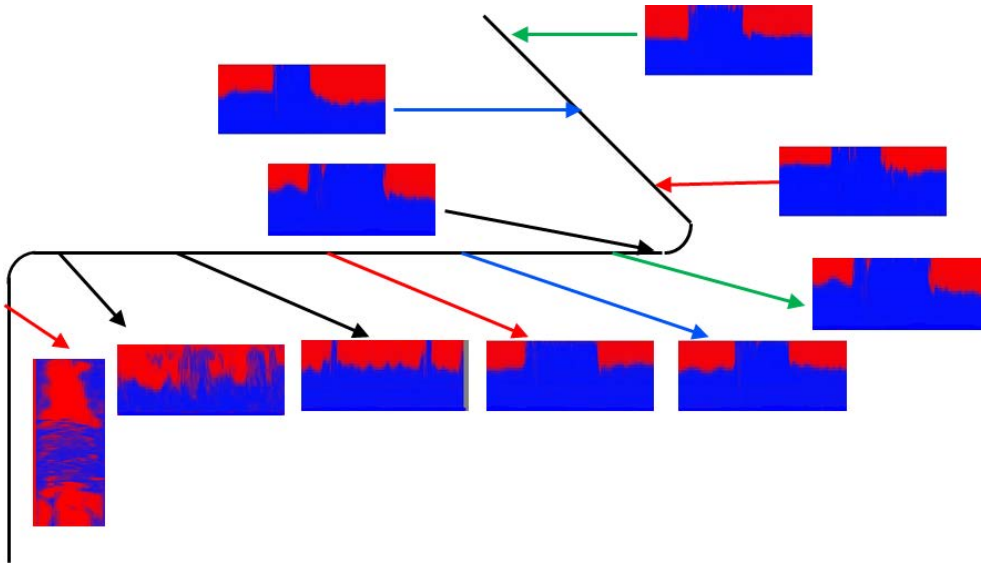

Fig.14 Tomographic images from positions along the pipe system. Liquid superficial velocity = 0.45 m/s and gas superficial velocity = 0.55 m/s.

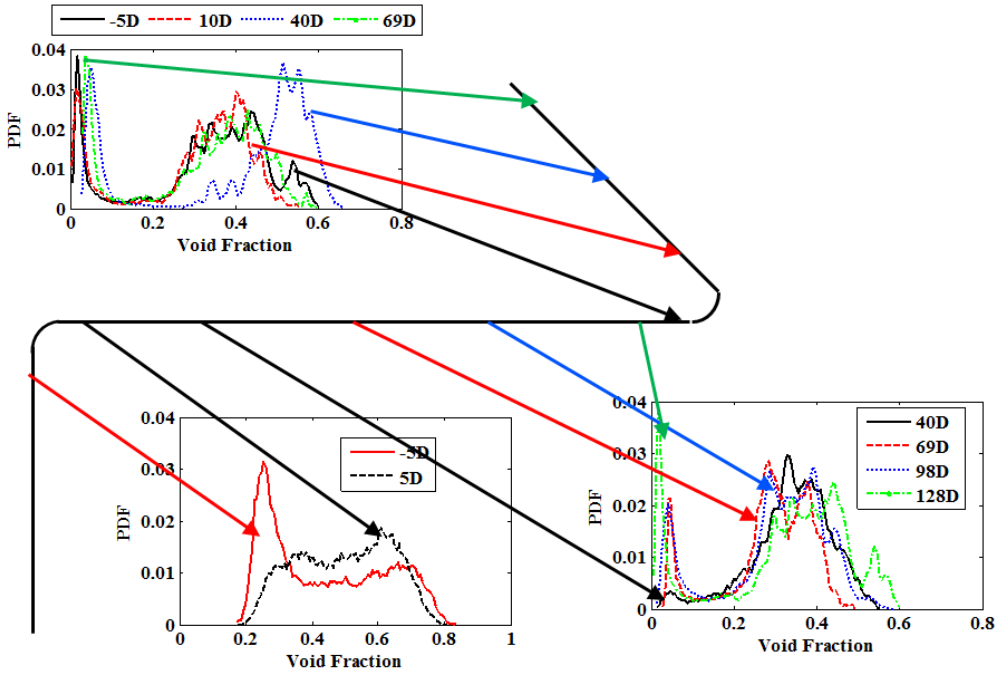

Fig.15 Probability Density Function of void fraction time series positions along the pipe system. Liquid superficial velocity = 0.45 m/s and gas superficial velocity = 0.55 m/s.

The characteristic frequencies of the time series of void fraction obtained at all the position studied have been extracted the Power Spectral density approach. These are shown in Figs. 16 and 17 and illustrate the effect of gas and liquid flow rates. Though in some cases there is a rise from just before to just after the vertical to horizontal bend, this is not always the case. The more dominant trend is the continuous decrease with downstream position. Beyond the horizontal to horizontal bend the frequency can be independent of position. These results are significantly different from those for the horizontal to vertical bend presented in Fig.10. They indicate that there is no persistence of frequency and reinforces the point that only occurs if a flow pattern, particularly slug flow is maintained across the bend. The vertical to horizontal bend destroys slug flow, at least temporarily. As noted above it can take ~55D for it to reoccur.

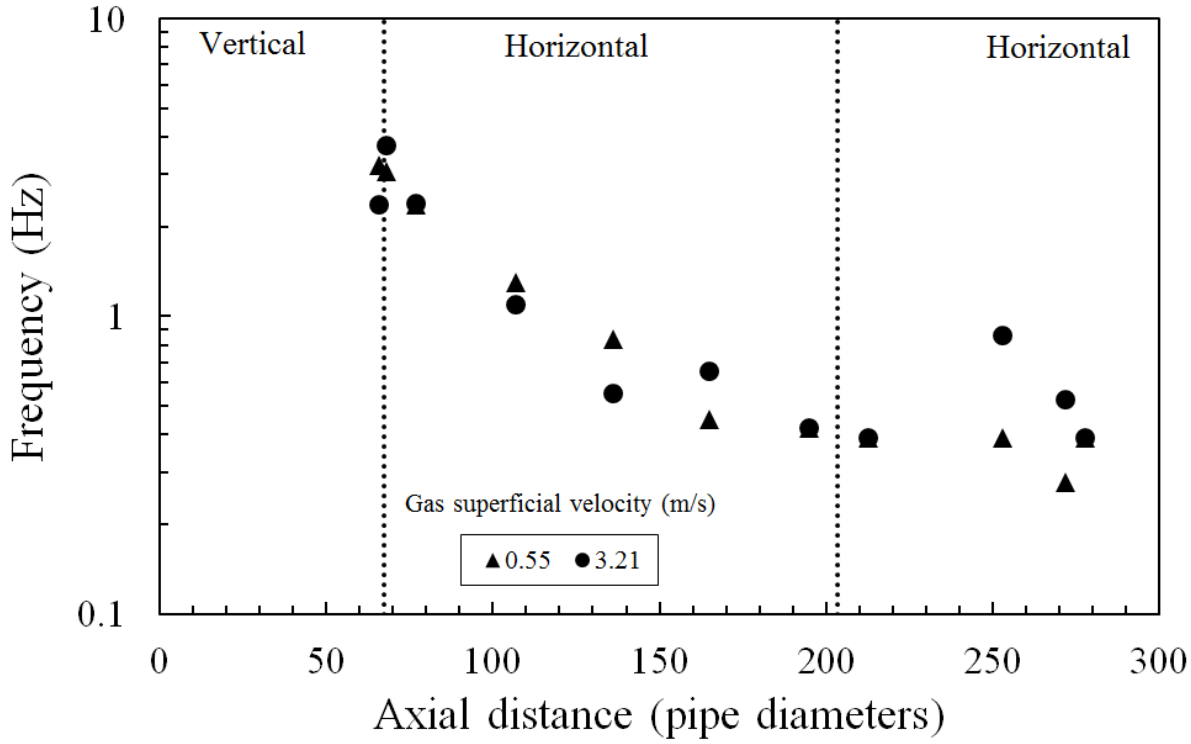

Fig.16 Characteristic frequency along the pipe system. Effect of gas flow rate. Liquid superficial velocity = 0.53 m/s.

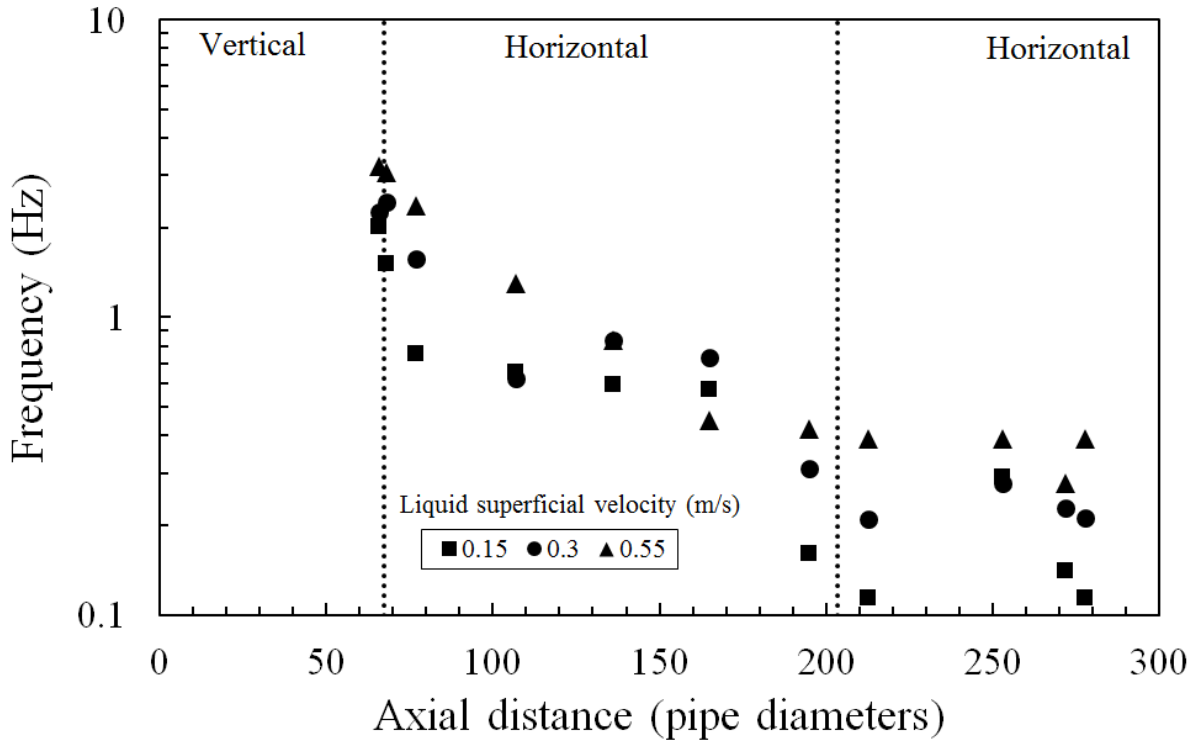

Fig.17 Characteristic frequency along the pipe system. Effect of liquid flow rate. Gas superficial velocity – 0.55 m/s.

4.4 180^o vertical inverted U-bend with 127mm ID

Liquid film thickness distribution of an air–water mixture flowing through a vertical inverted U-bend with 127mm ID was experimentally investigated. The water stored in the bottom of a separator was pumped to a gas–liquid mixer before it entered an 11 m vertical riser, flowed into the bend, went down a 9.6 m down-comer and returned to the separator. The riser has the same internal diameter as the bend and down-comer. The bend has a radius of curvature of 381 mm (R/D = 3) and consist of four modular blocks and one instrumentation section containing all the measuring sensors (parallel-ring probe, flush-mounted pin probe shown in Fig.4 and parallel-wire probe shown in Fig.5). This modular construction enables the measuring section to be inserted every 45^o along the bend. The superficial velocities of air ranged from 3.5 to 16.1 m/s and those for water from 0.02 to 0.2 m/s. At these superficial velocity ranges, churn and annular flows were dominated. More details about the rig and probe calibration can be found in [31, 35].

The variations of the liquid film thickness at a liquid superficial velocity of 0.2 m/s are shown in Fig.18. Here the values on the inside and outside of the bend only are shown together with value from upstream of the bend. In a previous publication [21], data were given in the form of polar coordinates but because the thin films involved, particularly on the outside of the bend, are so thin, these are not particularly informative.

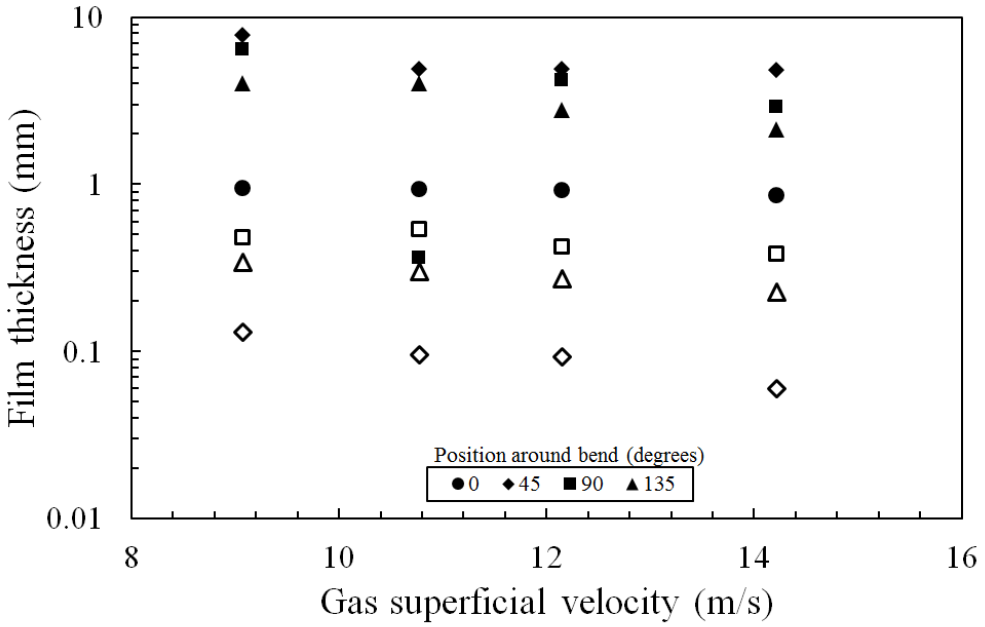

Fig.18 Variation of film thickness around the bend on the inside (closed symbols) and outside of the bend (open symbols). Liquid superficial velocity 0.2 m/s.

The plots show that the profile of the liquid film thickness changes significantly when the bend angle is increased from 45^o to 135^o. At the 90^o and 135^o bend positions, the liquid film is thick at the inside of the bend and of the same magnitude. The thick films become a source of new droplets and at the inside of the 90^o bend location; the liquid film is thinner than at the 45^o and 135^o bend designations. At the inside of the 45^o bend position, the liquid film is thicker than that at both the 90^o and 135^o bend positions. This may be due to the deposited droplets falling down owing to gravity drainage as a liquid film at the inside of the 45^o bend position. Though, a thickening of the liquid film outside the three bends is also visible, most especially at the 90^o and 135^o positions.

Because the ratio of average liquid film thickness to pipe diameter is very small, the variation of liquid film thickness cannot be seen clearly in the polar coordinates [21] the results are instead in Cartesian coordinates. Fig.19 shows the variation of the time averaged liquid film thickness that occurs in the bend. Here, the abscissa is the circumferential angular position of the probes and the 90 and 270^o are the top and bottom of the pipe. 0 and 180^o represent the side of the bend.

At a liquid superficial velocity of 0.1 m/s, the liquid film thickness inside the bend decreases with an increase in bend angle, 45^o to 135^o as shown in Fig.19a. In contrast, for the outside of the bend, the liquid film thickness increases and then slightly remains constant with an increase in bend angle. The increase in liquid film thickness on the inside of the 45^o bend can be attributed to gravity drainage which causes more liquid film to accumulate here. The increase on the other hand for the outside of the 90° and 135^o bends is a result of an increase

in droplet deposition outside the bend. This is in agreement with the observations reported by Flores *et al.* [43] who confirmed that a secondary flow exists in horizontal annular flow using a twin axial vorticity meter. The CFD calculations were carried out by Tkaczyk [44] using air and water and the same geometry as the experiments reported above. He employed Star-CD for the modelling and simulation of the air–water flow around a vertical 180^{o} return bend. The Star-CD code employs the Finite Volume method to numerically discretize the computational flow domain. The air–water flow was modelled as a continuum gas field, continuum liquid film and as liquid droplets of varying diameters. He accounted for the dynamics of the droplet flow in the gas core and the interaction between them. The liquid film was solved explicitly using a modified Volume of Fluid (VOF) method. The droplets were tracked using a Lagrangian technique. The liquid film to droplet and droplets to liquid film interactions were taken into account using sub-models to complement the VOF model. Tkaczyk [44] took into consideration the fact that in free surface flows, a high velocity gradient at the gas/liquid interface results in high turbulence generation. In order to overcome this inadequacy, he implemented a correction to the VOF model based on the work of Egorov [45]. Full details can be found in Tkaczyk [44]. The model gives a reasonably good prediction of the liquid film thickness in the bend. Fig. 19 shows the comparison between the experimental results and those obtained numerically. The film thickness is plotted on a logarithmic scale to show the variation of the lower film thicknesses more clearly. Tkaczyk [44] correctly predicted the liquid film thickness inside the 90 and 135^{o} bends at the liquid and gas superficial velocity of 0.1 and 14.8 m/s, respectively, but under-estimated the maximum film thickness inside the 45^{o} bend with an error of 65 %. It is interesting to note that the double peaks found on the liquid film thickness at the 45^{o} bend were correctly predicted by the model.

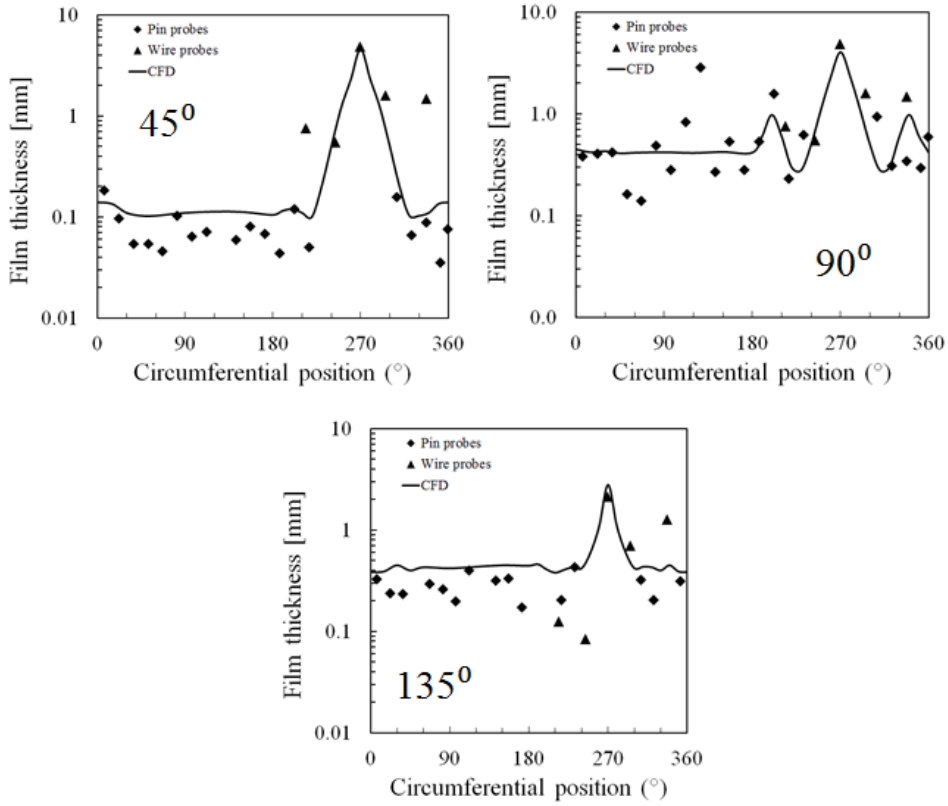

Fig.19 Spatial liquid film thickness distribution at liquid superficial velocity of 0.2 m/s and gas superficial velocity of 14.5 m/s.

For a liquid superficial velocity of 0.2 m/s, the maximum liquid film thicknesses for the inside of the bend are found at the 45^{o} position as shown in Fig.19. Now the impingement point for drops is beyond 45°. But by 90° this liquid has drained under gravity to the inside of the bend. In addition, some of the liquid meant to move up to the 90^{o} bend returned back (back flow) to the 45^{o} bend due to its lower momentum and curvature of the bend. According

to Abdulkadir *et al.* [21], these two scenarios could explain why the observed liquid film at the bottom of the 45^{o} bend was thicker than the other locations, at 90° and 135^{o}. Some of the liquid at the bottom and top of the 90^{o} bend due to the action of gravity and shape of the curvature of the bend, drain down to the bottom of the 135^{o} bend and accumulate there. Also the droplets that impinged on the wall also deposit at the 135^{o} bend. This could be the reason why there is a thick film at the 135^{o} bend but less than those found at the 45^{o} and 90^{o} bends. This claim is also supported by the images taken by a high speed video camera. For the outside of the bend scenario, the liquid film is thickest at the 90^{o}, followed by the 135^{o} and thinnest at the 45^{o} bend. The film is wavy. This indicates that more liquid is drained from the top of the 45^{o} bend. As a consequence of this drainage, the liquid film at the outside of the 45^{o} bend thins out and become more uniformly distributed around it. The uniformity of the liquid film outside the 45^{o} bend could be due to a balance of circumferential drag, shear and gravity forces. Another possible explanation could be that the pin probes limited to thin liquid film measurements failed to detect the thick films outside the 45^{o} bend.

The data collected can be used to understand the variation of liquid film thickness distribution with gas and liquid superficial velocities. This information can actually aid in providing information about where to locate a flow controller.

5. Conclusions

The knowledge of the phase distribution in the bends and the influence of the bends on flow downstream of them is crucial when a desired flow patterns need to be maintained in pipes. From the data provided, appropriate diameters could be suggested to achieve a specific flow pattern. The information presented provides useful guidance on where sensors driving flow controllers should be located. If there is a requirement to have or avoid slug flow, then a detector should be positioned just downstream of a vertical to horizontal bend. However, because slug flow can reform further downstream, a second detector ~100 D further

downstream might be sensible. It is noted that the full cross section distribution of the phases is not required. The approach proposed by Jeanmeure et al. [31} would be much simpler yet perfectly adequate. It could be adaptable for industrial applications. It employs capacitance measurements and is so is applicable only to non-conducting liquids. However, an equivalent version using resistance for conducting liquids such as water should be possible.

The material presented above has shown that state of the art instrumentation is required to extract the complexities of gas-liquid flows in bends. These instruments, though suitable for laboratory applications would need significant developments before they could be utilised in industrial applications. Therefore, the contribution of this work to the control of gas-liquid flows in bends will be limited to the passive type, where the knowledge influences the design of geometry employed and the flow rates used.

In the case of fired heaters, coking occurs is just before the bend. This is caused by the rate of entrainment of drops from the film and the rate of evaporation from the film is greater than the rate of replenishment of the film by depositing drops. A more important problem is the split of feed between tubes in parallel. If one of these tubes has a low flow, that is the one in which coking will occur.

The data provided in the paper will be useful in developing a fit-for-purpose phase separator. The bend/T-junction separators require the majority of the liquid on the outside of the bend in a steady manner, i.e., stratified flow is preferable to slug flow. The accumulated knowledge above will enable the optimum pipe diameter to be selected.

Acknowledgements

Elements of this work were carried out as part of grants from the UK Engineering and Physical Sciences Research Council (grant numbers EP/E004644/1 & EP/F016050/1).

This work has been undertaken within the Joint Project on Transient Multiphase Flows and Flow Assurance, sponsored by Advantica; BP Exploration; CD-adapco; Chevron; ConocoPhillips; ENI; ExxonMobil; FEESA; IFP; Institutt for Energiteknikk; Norsk Hydro; PDVSA (INTERVEP); Petrobras; PETRONAS; Scandpower PT; Shell; SINTEF; Statoil and TOTAL. The Authors wish to express their sincere gratitude for their support.

M. Abdulkadir would like to express sincere appreciation to the Nigerian government through the Petroleum Technology Development Fund (PTDF) for providing the funding for his doctoral studies. L.A. Abdulkareem would like to express sincere appreciation to the University of Zakho and the Ministry of Higher Education, Kurdistan Regional Government for providing the funding for his doctoral studies.

References

[1] Corder, S.B. The near-surface expansion of gas slugs: insights from laboratory experiments into eruptive activity at low-magma-viscosity volcanoes. PhD Thesis, Lancaster University, U.K. (2008).

[2] G. Sakamoto, T. Doi, Y. Murakami, K. Usui, Profiles of liquid film thickness and drop flow rate in U-bend annular mist flow. 5th International Conference on Multiphase Flow, Yokahama, May 30-June 4, paper Mo. 317 (2004).

[3] B.J. Azzopardi, Gas-liquid flows. New York: Begell House (2006).

[4] L.P. Golan, A.H. Stenning, Two-phase vertical flow maps. Proc. Inst. Mech. Engrs., 184 (1969) 108-114.

[5] T. Takemura, K. Roko, M. Shiraha, S. Midoriyama, S., Dryout characteristics and flow behaviour of gas-water two-phase flow through U-shaped and inverted U-shaped bends. Nucl. Eng. Design, 95 (1986) 365-373.

[6] L.Y. Chong, B.J. Azzopardi, D.J. Bate, . Calculation of Conditions at which dry out occurs in the Serpentine Channels of Fired Reboilers. Chem. Eng. Res. Des., 83 (2005) 412-422.

[7] G.F. Hewitt, A.H. Govan, Phenomenological modelling of non-equilibrium flow with phase change. Int. J. Heat Mass Trans., 32 (1990) 229-242.

[8] B.J. Azzopardi, D.A. Colman, D. Nicholson, D., Plant application of a T-junction as a partial phase separator. Chem. Eng. Res. Design, 80 (2002) 87-96.

[9] F. Sanchez-Silva, V. Hernandez-Perez, I. Carvajal-Mariscal, J.G. Barbosa-Saldaña, J.A. Cruz-Maya, Separation of a two-phase slug flow in branched 90 deg elbows. J. Fluids Eng., 132 (2010) 051301-1-051201-8.

[10] G. Baker, W. Clark, B.J. Azzopardi, J.A. Wilson, Controlling the phase separation of gas-liquid flows at horizontal T-junctions. AIChE Journal, 53 (2007) 1908-1915

[11] G. Baker, W. Clark, B.J. Azzopardi, J.A. Wilson, Transient effects in gas-liquid phase separation at a pair of T-junctions. Chem. Eng. Sci., 63 (2008) 968-976

[12] G.H. Anderson, P.D. Hills, Two-phase annular flow in tube bends. Symposium on Multiphase Flow Systems, University of Strathclyde, Glasgow, Paper J1. Published by Institution of Chemical Engineers Symposium, Series No. 38. (1974).

[13] J.D. Balfour, D.L.Pearce, Annular flows in horizontal 180^{o} bends: measurements of water rate distributions in the film and vapour core. C.E.R.L. Note No. RD/L/N96/78 (1978).

[14] K. Hoang, M.R. Davis, Flow structure and pressure loss for two-phase flow in round bends. J. Fluids Eng. 106 (1984) 30 -37

[15] Tingkuan, C., Zhihua, Y., and Qian, W., 1986. Two-phase flow and heat transfer in vertical U-shaped tubes (I) Flow pattern transitions in the bend. Journal of Chemical Industry and Engineering (China) 1, 1-12.

[16] J.M. Mandhane, G.A. Gregory, K. Aziz, A flow pattern map for gas-liquid flow in horizontal pipes. Int. J. Multiphase Flow 1 (1974) 537-553.

[17] J. Weisman, S.Y. King, Flow pattern transitions in vertical and upwardly inclined lines. Int. J. Multiphase Flow 7 (1981)271-291.

[18] P.W. James, Azzopardi, B.J., D.I. Graham, C.A. Sudlow, C.A., The effect of a bend on droplet distribution in two-phase flow. International Conference on Multiphase Flow in Industrial Plants, Bologna, 13-15 September (2000).

[19] M. Abdulkadir, D. Zhao, S. Sharaf, L. Abdulkareem, I.S. Lowndes, B.J. Azzopardi, Interrogating the effect of 90^o bends on air–silicone oil flows using advanced instrumentation, Chem. Eng. Sci. 66 (2011) 2453–2467.

[20] M. Abdulkadir, D. Zhao, A. Azzi, I.S. Lowndes, B.J. Azzopardi,. Two-phase air–water flow through a large diameter vertical 180^o return bend. Chem. Eng. Sci. 79 (2012) 138–152.

[21] M. Abdulkadir, A. Azzi, D. Zhao, I.S. Lowndes, B.J. Azzopardi, Liquid film thickness behaviour within a large diameter vertical 180^o return bend, Chem. Eng. Sci. 107 (2014) 137–148.

[22] T. Oshinowo, M.E. Charles, Vertical two-phase flow- Part 1: Flow pattern correlations. Can. J. Chem. Eng. 52 (1974) 25-35.

[23] K.D. Kerpel, T. D. Keulenaer, S. D. Schampheleire, M. D., Paepe, Capacitance sensor measurements of upward and downward two-phase flow in vertical return bends. Int. J. Multiphase Flow 64 (2014) 1-10.

[24] L.-C. Hsu, I.Y. Chen, C.-M. Chyu, C.-C. Wang, Two-phase pressure drops and flow pattern observations in 90^o bends subject to upward, downward and horizontal arrangements. Exp. Thermal Fluid Sci. 68 (2106) 484-492

[25] S. Yadav, H.B. Mehta, Experimental investigations of air–water two-phase flow through a minichannel U-bend. Exp. Thermal Fluid Sci., doi: http://dx.doi.org/10.1016/j.expthermflusci.2016.05.019 (2016)

[26] A.A. Almabrok, A.M. Aliyu, L. Lao, H. Yeung, Gas/liquid flow behaviours in a downward section of large diameter vertical serpentine pipes, Int. J. Multiphase Flow 78 (2016) 25-43.

[27] A. Almabrok, L. Lao, H. Yeung, Effect of 180° bends on gas/liquid flows in vertical upward and downward pipes, WIT Trans. Eng. Sci., 79 (2013) 435-445.

[28] S.M. Huang, Impedance sensors-dielectric systems. In: Williams, R.A., Beck, M.S. (Eds.), Process Tomography. Butterworth-Heinemann Ltd., Cornwall (1995).

[29] K. Zhu, S. Madhusudana Rao, C. Wang, S. Sundaresan, Electrical capacitance tomography measurements on vertical and inclined pneumatic conveying of granular solids. Chem. Eng. Sci. 58 (2003) 4225–4245.

[30] A. Hunt, J. Pendleton, M. Byars, Non-intrusive measurement of volume and mass using electrical capacitance tomography. In: Proceedings of the 7th Biennial ASME Conference on Engineering System Design and Analysis, Manchester, UK, ESDA 2004-58398 (2004).

[31] B.J. Azzopardi, V Hernandez Perez, R. Kaji, M.J. da Silva, M. Beyer, U. Hampel,. Wire Mesh Sensor Studies in a Vertical Pipe. Fifth International Conference on Transport Phenomena in Multiphase Systems, Bialystok, Poland (2008).

[32] L.A.Abdulkareem,. Tomographic Investigation of Gas–Oil Flow in Inclined Risers, PhD Thesis, University of Nottingham (2011).

[33] L.F.C. Jeanmeure, T. Dyakowski, W.B.J. Zimmerman, W. Clark, Direct flow-pattern identification using electrical capacitance tomography, Powder Technol. 112 (2000) 174-192.

[34] M.J. da Silva, S. Thiele, L.A. Abdulkareem, B.J. Azzopardi, U. Hampel, 2010. High-resolution oil-gas two-phase flow measurement with a new capacitance Wire-Mesh Tomography. Flow Meas. Instr. 21 (2010) 191-197.

[35] S. Sharaf, M. Da Silva, U. Hampel, C. Zippe, M. Beyer, B. Azzopardi, Comparison between wire mesh sensor technology and gamma densitometry, Meas. Sci. Tech. 22 (2011) 104019 (13 pp)
[36] B.J. Azzopardi, L.A. Abdulkareem, D. Zhao, S. Thiele, M.J. da Silva, M. Beyer, A. Hunt, Comparison between Electrical Capacitance Tomography and Wire Mesh Sensor output for air/silicone oil flow in a vertical pipe, *Ind. Eng. Chem. Res*. 49 (2010) 8805-8811.
[37] J.C. Asali, T.J. Hanratty, P. Andreussi, Interfacial drag and film height for vertical annular flow, AIChE J. 31 (1985) 895–902.
[38] P. Andreussi, A. Di Donfrancesco, M. Messia, 1988. An impedance method for the measurement of liquid hold-up in two phase flow, Int. J. Multiphase Flow 14 (1988) 777–85.
[39] N.A. Tsochatzidis T.D. Karapantios M.V. Kostoglou A.J. Karabelas,. A conductance method for measuring liquid fraction in pipes and packed beds. Int. J. Multiphase Flow; 5 (1992) 653–67.
[40] M. Fossa, Design and performance of a conductance probe for measuring liquid fraction in two-phase gas-liquid flow, Flow Meas. Inst., 9 (1998) 103–109.
[41] F. Saidj, R. Kibboua A. Azzi, N, Ababou, B.J. Azzopardi, Experimental investigation of air–water two-phase flow through vertical 90◦ bend, Exp. Thermal Fluid Sci. 57 (2014) 226–234.
[42] J.E. Koskie, I. Mudawar, W.G. Tiederman, Parallel wire probes for measurement of thick liquid films. Int. J. Multiphase Flow15 (1989) 521–530.
[43] G. Conte, B.J. Azzopardi, Film thickness variation about a T-junction. Int. J. Multiphase Flow 29 (2003) 305–325.
[44] R.J. Belt, On the liquid film in inclined annular flow. PhD Thesis, Delft University of Technology, Netherlands. (2006).
[45] G. Geraci, Inclination effects on circumferential film flow distribution in annular gas/liquid flows. AIChE Journal, 53 (2007) 5, 1144-1150; G. Geraci, Effect of inclination on circumferential film thickness variation in annular gas/liquid flow. Chem. Eng. Sci. 62 (2007) 3032- 3042.
[46] M.H.S. Zangana, Film behaviour of vertical gas–liquid flow in a large diameter pipe. Ph.D. Thesis, University of Nottingham, United Kingdom. (2011).
[47] M. Miya, Properties of roll waves. PhD Thesis, University of Illinois, Urbana, USA. (1970).
[48] M. Miya, D.E. Woodmansee, T.J. Hanratty, A model for roll waves in gas– liquid flow. Chem.Eng.Sci.26 (1971) 1915 – 1931.

Vitae

Dr Donglin Zhao is Senior Lecturer in Chemical Engineering in London South Bank University. He obtained PhD in chemical Engineering in the University of Surrey. He has more than 20 years' experience working in the areas of gas-liquid mixing, enhanced heat transfer and multiphase flow. He is a co-author of a book and published dozens of papers in refereed journals and conference proceedings.

Dr Abdulkadir Mukhtar has a PhD in Chemical Engineering from the University of Nottingham, United Kingdom. Currently, he is a senior lecturer in the Chemical Engineering Department, Federal University of Technology, Minna, Nigeria. He is also a visiting assistant

professor, Petroleum Engineering Department, African University of Science and Technology, Abuja, Nigeria. Dr. Abdulkadir is interested in multiphase flow research which finds applications in the oil/gas production, process and power sectors of industry. He also has research interests in the development of computational fluid dynamics models to characterize the complex phenomena exhibited by gas–liquid flows in straight pipes and bends.

Dr Lokman A Abdulkareem is Dean of the Faculty of Engineering at the University of Zakho. He received Ph.D. in Chemical engineering from the University of Nottingham/ United Kingdom. He has more than 18 years experience of academic teaching and research. His research projects are involving the application of advanced tomographic instrumentation such as Electrical Capacitance Tomography and wire mesh sensor. He has led many research grants and contracts funded by institutions and Industry. In addition, he has been a member of Master projects panels at some institutions. He teaches many modules in different universities and institutes. He has published over 40 articles in refereed journals, conference proceedings, and other edited collections.

Dr Abdelwahid Azzi is Professor in Mechanical Engineering at the University of Sciences and Technology Houari Boumedien, Algiers (USTHB). He carried a large part of his PhD thesis at the Technical University of Hamburg Harburg (TUHH), Germany. For several years, he led the Two-phase flow group in the Multiphase Flow and Porous Media Laboratory (USTHB). From 2006, he started his research collaboration with Prof. B.J. Azzopardi from the University of Nottingham. During his several research stays at this University, sponsored by the EPSRC as well the Algerian Ministry of High Education and Research, he worked on several projects: all in the multiphase flow area.

Dr Faiza Saidj is Lecturer in Process Engineering at the University of Sciences and Technology Houari Boumedien, Algiers (USTHB). She started her research career by preparing a Master degree in chemical engineering. This research work were dealing with oil extraction from plants. The results of these investigations have been published in journal papers and conferences. In 2010, she joined the Multiphase Flow and Porous Media Laboratory, to carry out her PhD research thesis. In 2015, she received her PhD degree from the same university. Her research thesis concerned the analysis of two-phase flow behaviour in vertical 90° bend. Actually, she is working on topics all of them in two-phase flow area.

Dr Valente Hernandez-Perez is a research fellow in the Mechanical Engineering Department, National University of Singapore, Singapore, within the Centre for Offshore Research Engineering (CORE). He worked previously as a research fellow at Nottingham University, United Kingdom. Dr. Hernandez-Perez obtained his PhD in Chemical Engineering from the University of Nottingham, United Kingdom. His research has been focused on multiphase flow (mainly gas-liquid) by means experimental and computational methods.

Mr. Rajab Omar completed the BSc. degree in chemical engineering from Al-Zawia University, Libya. He received the MSc in Chemical Engineering from the University of Nottingham, UK in 2011. Currently he is conducting research on transitional two phase flows around 90° bends in The University of Nottingham for a PhD degree in chemical engineering.

Dr. Buddhi Hewakandamby has a PhD in Chemical Engineering from the University of Sheffield. Currently, he is an assistant professor in the Department of Chemical and Environmental Engineering, University of Nottingham, United Kingdom. His research

interests include multiphase flows phenomena across various length scales, flow instabilities, flow with heat transfer and CFD modelling.

Barry Azzopardi is Lady Trent Professor of Chemical Engineering at the University of Nottingham. He is the author of two books and more than 300 refereed papers on aspects of multiphase flow. He has designed and operated very large experimental facilities and applied state of the art instrumentation to multiphase flow, particularly electrical tomography. He has worked on drops and films in annular flow, bubbly, slug and most recently churn flows. As well as working on pipe flows he is recognised as an expert on venturis and T-junctions as well as bends.